THE JOURNAL OF BIOLOGICAL CHEMISTRY VOL. 286, NO. 27, pp. 24467–24475, July 8, 2011

Dependence on Endocytic Receptor Binding via a Minimal Binding Motif Underlies the Differential Prognostic Profiles of SerpinE1 and SerpinB2 in Cancer*[S]

Received for publication, January 27, 2011, and in revised form, May 13, 2011 Published, JBC Papers in Press, May 23, 2011, DOI 10.1074/jbc.M111.225706

Blake J. Cochran[‡§1], **David R. Croucher**[¶], **Sergei Lobov**[‡2], **Darren N. Saunders**[¶], **and Marie Ranson**[‡§3]

From the [‡]*School of Biological Sciences and* [§]*Illawarra Health and Medical Research Institute, University of Wollongong, Wollongong, New South Wales 2522, Australia and the* [¶]*Cancer Research Program, Garvan Institute of Medical Research, Sydney, New South Wales 2010, Australia*

Tumor overexpression of urokinase-type plasminogen activator (uPA) and its specific inhibitor SerpinE1 (plasminogen activator inhibitor type-1) correlates with poor prognosis and increased metastatic potential. Conversely, tumor expression of uPA and another specific inhibitor, SerpinB2 (plasminogen activator inhibitor type-2), are associated with favorable outcome and relapse-free survival. It is not known how overexpression of these uPA inhibitors results in such disparate outcomes. A possible explanation may be related to the presence of a proposed low density lipoprotein receptor (LDLR)-binding motif in SerpinE1 responsible for mitogenic signaling via ERK that is absent in SerpinB2. We now show that complementation of such a LDLR-binding motif in SerpinB2 by mutagenesis of two key residues enabled high affinity binding to very LDLR (VLDLR). Furthermore, the VLDLR-binding SerpinB2 form behaved in a manner indistinguishable from SerpinE1 in terms of enhanced uPA-SerpinB2 complex endocytosis and subsequent ERK phosphorylation and cell proliferation; that is, the introduction of the LDLR-binding motif to SerpinB2 was necessary and sufficient to allow it to acquire characteristics of SerpinE1 associated with malignancy. In conclusion, this study defines the structural elements underlying the distinct interactions of SerpinE1 *versus* SerpinB2 with endocytic receptors and how differential VLDLR binding impacts on downstream cellular behavior. This has clear relevance to understanding the paradoxical disease outcomes associated with overexpression of these serpins in cancer.

SerpinE1 (plasminogen activator inhibitor type-1, PAI-1)[4] and SerpinB2 (plasminogen activator inhibitor type-2, PAI-2) are both efficient inhibitors of the urokinase-type plasminogen activator (uPA), a key enzyme in the tissue remodeling process. Combined tumor overexpression of uPA, its receptor (uPAR), and SerpinE1 (serine protease inhibitor E1) is strongly correlated with poor patient prognosis (1–3) and metastatic potential (4–8). Consequently, uPA and SerpinE1 expression is recommended as an independent prognostic indicator in node-negative breast cancer (9). On the contrary, tumor expression of SerpinB2 is correlated with increased relapse-free survival in breast cancer (and possibly other cancer types) (10). Further, the relationship between outcome and high SerpinB2 levels in node-negative breast cancer is only relevant if uPA levels are also elevated (1, 11), suggesting that the inhibitory relationship between uPA and SerpinB2 mediates this functionality.

Binding of uPA to uPAR has been reported to induce the activation of numerous cell type-specific signaling pathways, such as MAPK/ERK, JAK/STAT, Src, focal adhesion kinase, and Rac, thereby affecting cell adhesion, migration, differentiation, and apoptosis (12). Because uPAR is not a transmembrane protein, being linked to the cell surface by a glycosylphosphatidylinositol anchor, uPA/uPAR signaling is mediated by integrins and several other adaptor molecules, including members of the low density lipoprotein receptor (LDLR) superfamily (12–15). Both SerpinE1 and SerpinB2 efficiently inhibit uPA in solution and at the cell surface (16–18) through the formation of covalent, irreversible enzyme-substrate complexes. Following the formation of an inhibitory complex at the cell surface, uPA-Serpin complexes are rapidly cleared via LDLR-mediated endocytosis (18–21). Inhibition of uPA by SerpinE1 has previously been shown to modulate uPA/uPAR signaling, resulting in sustained activation of the MAPK/ERK signaling pathway in both MCF-7 and SGC7901 cells (22, 23), leading to increased cell growth (23) and expression of MMP-2 and MMP-9 (22) in these cell lines, respectively. Webb *et al.* (23) demonstrated that this promitogenic activity was dependent on the direct, high affinity interaction between the SerpinE1 moiety of the uPA-SerpinE1 complex and the very low density lipoprotein receptor (VLDLR). We have previously demonstrated that SerpinB2 does not initiate these signaling events following uPA inhibition and VLDLR-mediated endocytosis (21), and SerpinB2 (unlike SerpinE1) does not bind directly to LDLRs (20, 21).

* This work was financially supported by an Australian Postgraduate Award (to B. J. C.), by the University of Wollongong through the Centre for Medical Bioscience, by a University of Wollongong Small Grant, and by Cancer Institute New South Wales Fellowships (to M. R., D. N. S., and D. R. C.).

[S] The on-line version of this article (available at http://www.jbc.org) contains supplemental text and Figs S1 and S2.

[1] Present address: Lipid Research Group, The Heart Research Institute, Newtown, NSW 2042, Australia.

[2] Present address: Research School of Physics and Engineering, The Australian National University, Canberra, ACT 0200, Australia.

[3] To whom correspondence should be addressed: Illawarra Health and Medical Research Institute, University of Wollongong, NSW 2522, Australia. Tel.: 61242213291; E-mail: mranson@uow.edu.au.

[4] The abbreviations used are: PAI, plasminogen activator inhibitor; LDLR, low density lipoprotein receptor; uPA, urokinase plasminogen activator; uPAR, urokinase plasminogen activator receptor; VLDLR, very low density lipoprotein receptor; RAP, receptor-associated protein.

Additionally, the affinity and mechanism of interaction between uPA-SerpinB2 complex and LDLRs is markedly different from that of uPA-SerpinE1 (20, 21, 24). Numerous studies have identified several positively charged residues within (Lys^{69}, Arg^{76}, and Lys^{80}) and nearby (Lys^{88}, Arg^{118}, and Lys^{122}) α-helix D of SerpinE1 that contribute to the high affinity binding of uPA-SerpinE1 with LDLRs (24–27). In addition, α-helix D of SerpinE1 contains a proposed LDLR minimal binding motif consisting of two basic residues (Arg^{76} and Lys^{80}) separated by two to five residues and *N*-terminally flanked by hydrophobic residues (Leu^{75} and Tyr^{79}) (28) (see Fig. 1*A*). Our previous analysis suggested that the decreased affinity of uPA-SerpinB2 may be due to an incomplete LDLR-binding motif within α-helix D of SerpinB2, in which the first hydrophobic/basic amino acid pair is conserved, whereas the second pair is replaced by serine residues (21) (see Fig. 1*A*). Indeed, previous studies using a mutant form of SerpinE1 with an incomplete LDLR-binding motif (R76E) observed decreased LRP1 (low density lipoprotein receptor related protein-1) and VLDLR binding affinity and hence functional outcomes (21, 23, 25). We hypothesized that SerpinB2 may inhibit and clear cell surface uPA (and hence proteolytic activity) without influencing the promitogenic signaling pathways activated via SerpinE1, thus accounting for the differential prognosis associated with the expression of these serpins in tumors (10, 21). Herein, we show that VLDLR and LRP1 binding can be introduced to SerpinB2 by complementation of the LDLR-binding motif within α-helix D. This has profound impact on the functionality of SerpinB2.

EXPERIMENTAL PROCEDURES

Materials—QuikChange site-directed mutagenesis kit was from Stratagene (La Jolla, CA). The Alexa 488 labeling kit and Alexa 488 quenching polyclonal antibody were from Invitrogen (Carlsbad, CA). Z-Gly-Gly-Arg-AMC was from Calbiochem (San Diego, CA). HMW-uPA was from American Diagnostica (Stamford, CT). Protease inhibitor mixture, glutamine, transferrin, and selenium were from Sigma-Aldrich. SerpinE1 14-1B stable mutant and purified human receptor-associated protein (RAP) were from Molecular Innovations (Novi, MI). Antibodies to ERK and phosphorylated ERK were from Cell Signaling Technology (Danvers, MA). The recombinant human VLDLR ligand-binding region (V1–V7) was a gift from Prof. Dieter Blass (University of Vienna, Vienna, Austria). Human purified placental LRP1 was a kind gift from Prof. Phillip Hogg (University of New South Wales, Sydney, Australia). Both VLDLR and LRP1 were ≥95% pure as determined by SDS-PAGE (data not shown).

Cell Lines—The human breast adenocarcinoma (MCF-7) and human prostate carcinoma (PC-3) cell lines were obtained from American Type Culture Collection (Manassas, VA) distributed by Cryosite (Sydney, Australia). All of the cell lines were routinely cultured as previously described (21, 29). The cells were routinely tested for the absence of mycoplasma contamination and reconfirmed for the presence of VLDLR and absence of LRP1 (MCF-7) or vice versa (PC-3) as well as for the presence of uPAR by immunofluorescence staining as previously described (20, 21). Both cell lines also express negligible levels of either Serpin (20, 21).

Protein Structure Modeling—Molecular modeling and figure preparation was performed using structural coordinates obtained from x-ray crystal structures of the relaxed conformations of SerpinE1 (30) (Protein Data Bank code 9PAI) and SerpinB2 ΔCD-loop (31) (Protein Data Bank code 2ARQ) and PyMol (DeLano Scientific, Palo Alto, CA).

Site-directed Mutagenesis of SerpinB2 ΔCD-loop—Residues of SerpinB2 were replaced with the corresponding residues of SerpinE1 on the pQE9/SerpinB2 ΔCD-loop backbone (29), with the QuikChange site-directed mutagenesis kit using the following mutagenic primers (paired with their complements): D101K, 5′-GAAGTGGGAGCCGCTGCAAAGAAAATCCATTCATCCTTCC-3′; S111Y, 5′-CATTCATCCTTCCGCTCTCTCTATAAGGCAATCAATGCATCCAC-3′; S112K, 5′-CATCCTTCCGCTCTCTCAGCAAGGCAATCAATGCATCCACAGG-3′; and N120K, 5′-CAATCAATGCATCCACAGGGAAGTATTTACTGGAAAGTGTCAATAAG-3′. Each construct was confirmed by DNA sequencing before expression in *Escherichia coli* and purification as previously described (29). The SerpinB2 ΔCD-loop backbone was used for all SerpinB2 forms because removal of the CD-loop of SerpinB2 allows for easier purification of protein without compromising the inhibitory activity or LDLR binding affinity of SerpinB2 (29).

Preparation of uPA-Serpin Complexes uPA—Serpin complexes were prepared as previously described (23). Briefly, uPA and SerpinE1 or SerpinB2 forms were incubated at a 1:1 molar ratio for 30 min at 37 °C. Fractionation of samples of complexes by SDS-PAGE confirmed the presence of uPA-Serpin complexes with minimal/negligible residual-free protease or Serpin (data not shown).

Surface Plasmon Resonance—Surface plasmon resonance was performed essentially as previously described (20, 21, 29). VLDLR or LRP1 were loaded onto CM5 BIAcore sensor chips to a level of ~2000 response units. Analytes were diluted into BIAcore running buffer (10 mM Hepes, pH 7.4, 150 mM NaCl, 1 mM $CaCl_2$, 0.005% Tween 20) and run over the chip at 20 μl/min. Between samples, the sensor surface was regenerated with 100 mM H_3PO_4. The data were analyzed using BIAevaluation software (Version 4), using a blank cell as the reference cell. Where multiple CM5 chips were used, the results were validated against control chips and samples to ensure reproducibility.

Far-UV Circular Dichroism Spectrometry—The proteins were buffer-exchanged by dialysis into 10 mM sodium phosphate immediately prior to analysis and diluted to a concentration of 0.4 mg/ml. Far-UV circular dichroism spectrometry was performed using a J-810 spectropolarimeter (Jasco, Easton, MD) equipped with a thermoelectric temperature control at 25 °C. The spectra were collected from 190 to 240 nm at 0.1-nm intervals, with each spectrum representing the average of 10 scans and a sample of 10 mM sodium phosphate serving as a reference.

Activity Assay—Several substrate and uPA concentrations were used to find the optimum range and to set the gain on a Fluorostar Optima fluorescence plate reader (BMG Labtech). SerpinB2 samples were diluted in reaction buffer (20 mM Hepes, pH 7.6, 100 mM NaCl, 0.5 mM EDTA, 0.01% (v/v) Tween

20) and mixed with fluorogenic substrate, Z-Gly-Gly-Arg-AMC, in 180 μl of reaction buffer. After a brief preincubation at 37 °C, HMW-uPA (final concentration, 0.675 nM) was added to start the reaction, and fluorescence emission was measured immediately at 37 °C. All of the assays were performed in triplicate, and the values were corrected by subtracting the background (reaction buffer plus substrate only).

Endocytosis Assay—Cell internalization of $Alexa_{488}$-labeled uPA alone or in complex with either SerpinE1 or SerpinB2 forms was conducted in the absence or presence of the LDLR antagonist RAP (to confirm the involvement of LDLRs in this process) essentially as described previously (21, 29).

Analysis of ERK Activation—Activation of ERK was analyzed as described previously (23). MCF-7 cells were grown in 12-well plates to ~60% confluency and serum-starved for 12 h. The cells were incubated with 10 nM uPA or uPA-Serpin complexes for the time periods indicated. The cells were lysed with radioimmune precipitation assay buffer (50 mM Hepes, pH 7.4, 100 mM NaCl, 1% (v/v) Nonidet P-40, 2 mM EDTA, 0.4 mg/ml sodium orthovanadate, 5 mg/ml dithiothreitol, 1 ml/L protease inhibitor mixture), electrophoresed on 12% SDS-PAGE gels, transferred to PVDF membranes, and probed with antibodies that detect phosphorylated and total ERK.

Cell Proliferation Assay—Cell proliferation was examined in real time using the xCELLigence RTCA DP System (Roche Applied Science). The xCELLigence system allows continuous quantitative monitoring of cellular behavior including proliferation by measuring electrical impedance. MCF-7 cells were seeded at 5000 cells/well into E-Plate 16-well plates and cultured for 24 h. The medium was replaced with 100 μl of serum-free RPMI containing 300 μg/ml glutamine, 5 μg/ml transferrin, and 38 nM selenium in the presence of 10 nM uPA, uPA-Serpin complexes, or medium alone. Proliferation was continuously monitored every 15 min over a time period of 72 h. Data analysis was carried out using RTCA Software 1.2.1 supplied with the instrument.

Statistical Analyses—Statistical significance of treatment groups as compared with control groups was determined using an unpaired Student's *t* test (GraphPad Prism V 5.1; GraphPad Software, San Diego, CA). *p* values of <0.05 were considered statistically significant.

RESULTS

Structural Comparison Indicates Absence of a Consensus LDLR-binding Motif in SerpinB2—The surface charge and topology of the region defining the consensus LDLR-binding motif on α-helix D of SerpinE1 are clearly different from the corresponding region of SerpinB2 (Fig. 1, *B–E*). Hence, the differential binding to LDLRs and subsequent functional effects of SerpinE1 and SerpinB2 may be due to an incomplete LDLR-binding motif within SerpinB2 (10). To directly investigate this, we substituted residues of SerpinB2 with those corresponding to either the LDLR-binding motif within α-helix D of SerpinE1 and/or others previously identified as important for LDLR binding within or adjacent to α-helix D of SerpinE1 (24–26, 32) (Fig. 1, *A–C*). These residues were introduced into SerpinB2 ΔCD-loop in a stepwise manner to generate relevant single or compound mutants defined as indicated in Fig. 1*A*. Substitution of Ser^{111} and Ser^{112} in SerpinB2 with tyrosine and lysine, respectively (corresponding to Tyr^{79} and Lys^{80} in SerpinE1), to generate $SerpinB2^{YK}$ completed a potential LDLR minimal binding motif in SerpinB2 (Fig. 1*A*). $SerpinB2^{YK}$ and other mutants retained relative secondary structure and full inhibitory activity (supplemental Figs. S1 and S2).

Biochemical Characterization of LDLR-binding SerpinB2 Mutants—The panel of SerpinB2 mutants described in Fig. 1*A* were first assessed for their ability to bind directly to VLDLR using surface plasmon resonance methodology (Fig. 2). As previously demonstrated (21), SerpinB2 alone did not interact with VLDLR (Fig. 2*A*). VLDLR binding was also not observed for SerpinB2 mutants with incomplete LDLR minimal binding motifs (*i.e.* $SerpinB2^{K1}$, $SerpinB2^{K2}$, or $SerpinB2^{KK}$) (Fig. 2*A*). Urokinase-independent binding to VLDLR was only achieved by SerpinB2 mutants containing a complete LDLR minimal binding motif (*i.e.* $SerpinB2^{YK}$ and $SerpinB2^{KYK}$) (Fig. 2*A*). Dose-dependent kinetic analysis gave affinity constants (K_D) of 37.3 and 50.1 nM for $SerpinB2^{YK}$ and $SerpinB2^{KYK}$, respectively (Table 1).

Kinetic analyses of VLDLR interactions with uPA-SerpinB2 (Fig. 2*B* and Table 1) or uPA-$SerpinB2^{K2}$ and uPA-$Serpin^{KK}$ (data not shown) confirmed the single-site binding model anticipated for uPA complexes incorporating non-VLDLR binding SerpinB2 forms (21). In contrast, the interactions between VLDLR and uPA complexes incorporating the VLDLR binding $SerpinB2^{YK}$ or $SerpinB2^{KYK}$ forms were best described by a heterogeneous analyte model with two independent, competing binding sites on the complex with K_D values of 1.35 and 70.1 nM for uPA-$SerpinB2^{YK}$ and 1.53 and 51.2 nM for uPA-$SerpinB2^{KYK}$ (Fig. 2, *C* and *D*, and Table 1). As previously observed (21), uPA-SerpinE1 also best fits this binding model for interaction with VLDLR (Fig. 2*E*) and gave K_D values similar to those observed for uPA-$SerpinB2^{YK}$ and uPA-$SerpinB2K^{YK}$ (Table 1).

We have previously compared the differential binding interactions of uPA-SerpinE1 and uPA-SerpinB2 with a related LDLR family member, LRP1 (20). Again, although SerpinB2 alone did not bind (data not shown), kinetic analyses of uPA-SerpinB2 binding to LRP1 confirmed the single site binding model interaction (K_D = 1.02 nM) (Fig. 3*A* and Table 2). Interestingly, unlike that seen for VLDLR binding, the interaction between the uPA-$SerpinB2^{YK}$ complex and LRP1 displayed kinetics different from those observed for uPA-SerpinE1 (uPA-SerpinE1 K_D = 0.252 and 2.13 nM; uPA-$SerpinB2^{YK}$ K_D = 0.808 and 57.8 nM) (Fig. 3*B* and Table 2). Because Skeldal *et al.* (24) found that Lys^{88} of SerpinE1 (referred to as Lys^{90} in their study) is critical for the interaction between uPA-SerpinE1 and LRP1 (but not VLDLR), we generated an additional mutant ($SerpinB2^{YKK}$) replacing the asparagine at position 120 (corresponding to Lys^{88} of SerpinE1) with lysine (Fig. 1*A*). The uPA-$SerpinB2^{YKK}$ complex displayed strikingly similar LRP1 binding affinities to uPA-SerpinE1, with the high and lower affinity interactions (K_D = 0.128 and 2.72 nM) not significantly different from those of uPA-SerpinE1 (Table 2). However, it should be noted that individual k_a and k_d values were significantly different (Fig. 3, *C* and *D*, and Table 2), indicating subtle differences in interaction mechanics that may reflect variations in local surface potential and/or steric effects. Importantly, these

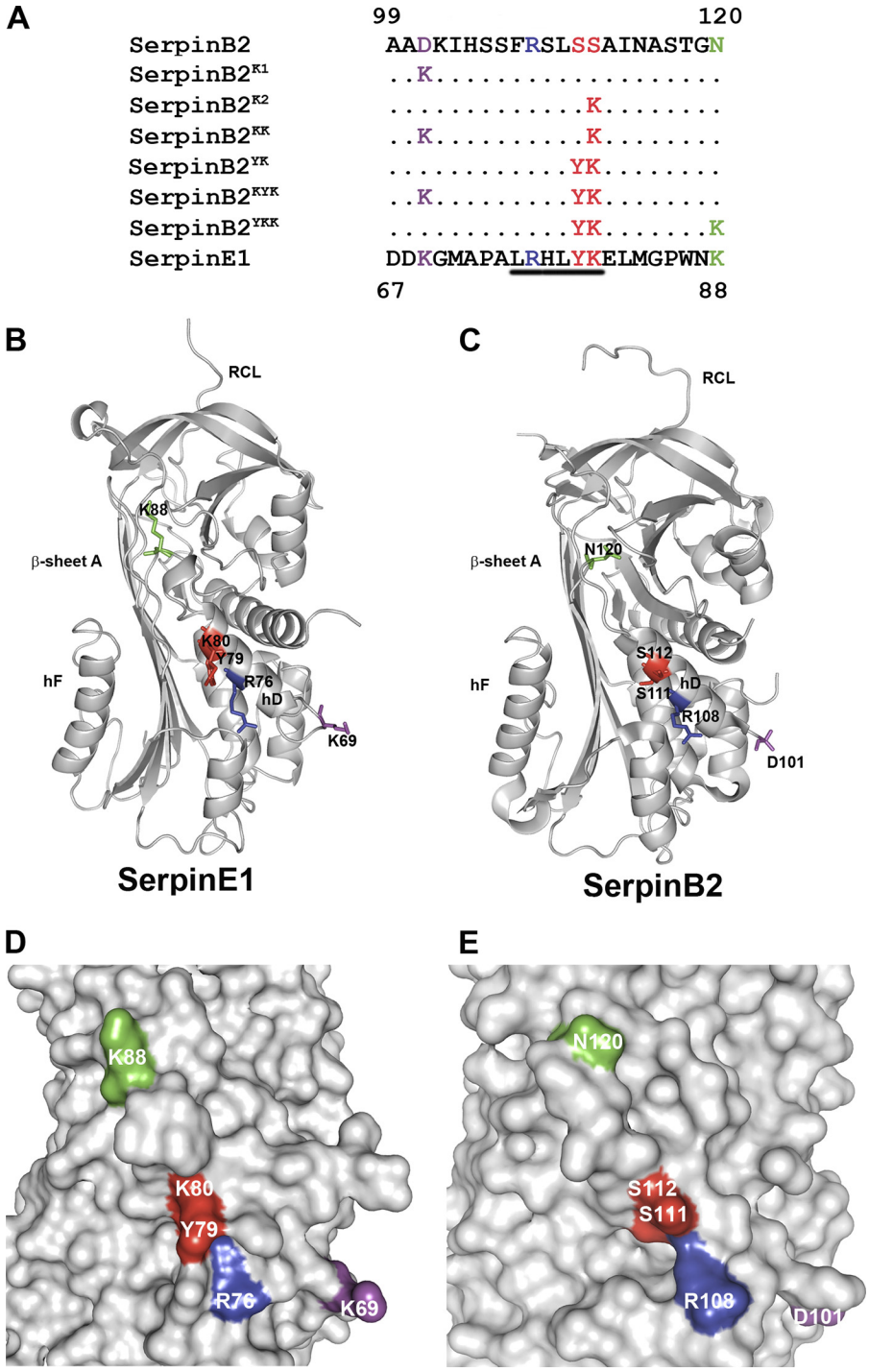

FIGURE 1. **Structural modeling of SerpinE1 and SerpinB2.** *A*, amino acid sequence alignment of the area in and adjacent to α-helix D of SerpinE1 and SerpinB2. The proposed LDLR minimal binding motif in SerpinE1 is *underlined*. Residues reported to be important for the interaction between SerpinE1 and LDLRs (24–27), and the corresponding residues in SerpinB2 are *colored*. The colored residues in SerpinB2 were mutated as indicated, resulting in the single and compound mutant forms that were utilized in this study. All of the SerpinB2 forms were constructed on the SerpinB2 ΔCD-loop backbone. *B–E*, ribbon representation (*B* and *C*) and surface representations (*D* and *E*) of the relative locations of SerpinE1 residues implicated in LDLR binding and the corresponding residues in SerpinB2. Analysis was performed using PyMol, SerpinE1 (Protein Data Bank code 9PAI) (30), and SerpinB2 ΔCD-loop (Protein Data Bank code 2ARQ) (31).

differences had negligible impact on overall binding affinities and downstream functional outcomes (see below).

Introduction of LDLR Binding to SerpinB2 Increased uPAR-mediated Endocytosis—We previously demonstrated that the affinity of uPA-Serpin complex for LDLRs is a key determinant of its rate of endocytosis (21), and we again observed significantly more uPA-SerpinB2 endocytosis (~4-fold, relative to uPA alone) by MCF-7 cells in an LDLR antagonist (RAP)-sensitive manner over a 30-min time period (Fig. 4*A*). Given that VLDLR is the only LDLR family member expressed by MCF-7 cells, these data reflect the increased affinity of the complex for VLDLR (Table 1). Accordingly, the RAP-sensitive endocytosis

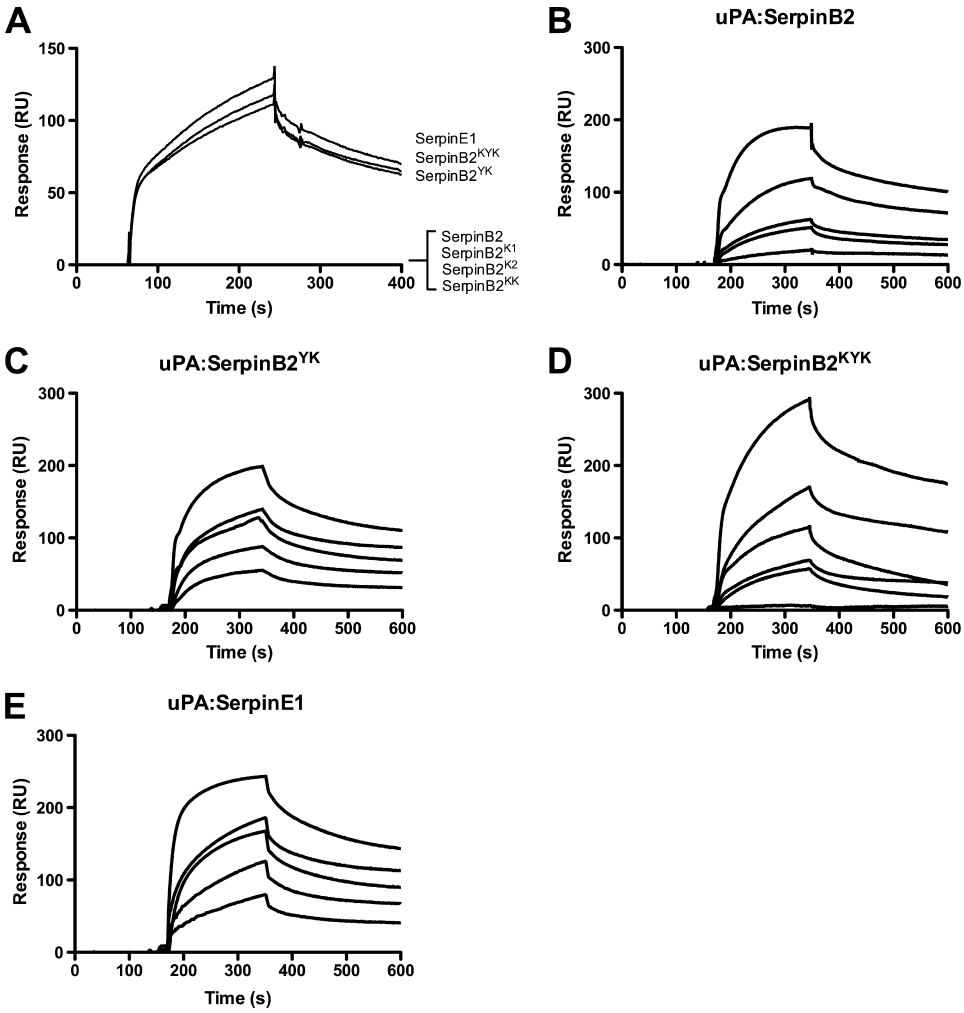

FIGURE 2. **Surface plasmon resonance analysis of the interaction between SerpinB2 constructs, SerpinE1, and VLDLR.** *A*, screening of SerpinB2 mutants for VLDLR binding. Surface plasmon resonance sensograms showing the interaction between 100 nM SerpinB2 mutants or SerpinE1 and immobilized VLDLR. The data shown are representative of at least three independent experiments. *B–E*, surface plasmon resonance analysis of the dose-dependent interaction between uPA complexed SerpinB2 mutants or uPA-SerpinE1 and VLDLR. The data presented here are representative of at least three experiments with analyte concentrations from 100 to 6.25 nM. All of the SerpinB2 forms were constructed on the SerpinB2 ΔCD-loop backbone.

TABLE 1

Kinetic parameters of the interaction between SerpinB2 forms used in this study and the endocytosis receptor VLDLR

The values were determined using surface plasmon resonance. The binding data were fitted using BIAevaluation 4.0 software. The binding model chosen represents that with the lowest χ^2 value. (The values are the averages ± S.E., $n \geq 3$). All of the SerpinB2 forms were constructed on the SerpinB2 ΔCD-loop backbone.

Analyte	Binding model	k_a	k_d	K_D	χ^2
		$M^{-1}\,s^{-1}$	s^{-1}	nM	
SerpinB2	No binding				
SerpinB2^{K1}	No binding				
SerpinB2^{K2}	No binding				
SerpinB2^{KK}	No binding				
SerpinB2^{YK}	1:1	6.77×10^4 ($\pm 2.68 \times 10^4$)	1.99×10^{-3} ($\pm 0.76 \times 10^{-3}$)	37.3 (±7.0)	0.97
SerpinB2^{KYK}	1:1	6.68×10^4 ($\pm 2.91 \times 10^4$)	4.31×10^{-3} ($\pm 2.22 \times 10^{-3}$)	50.1 (±10.2)	1.02
SerpinE1	1:1	8.98×10^4 ($\pm 2.1 \times 10^4$)	3.51×10^{-3} ($\pm 1.97 \times 10^{-3}$)	45.3 (±11.7)	5.9
uPA-SerpinB2	1:1	4.16×10^5 ($\pm 1.80 \times 10^5$)	1.36×10^{-3} ($\pm 0.23 \times 10^{-3}$)	4.30 (±0.56)	3.28
uPA-SerpinB2^{YK}	Heterogeneous analyte	4.78×10^4 ($\pm 0.38 \times 10^4$)	3.15×10^{-5} ($\pm 1.07 \times 10^{-5}$)	1.35 (±0.41)	7.6
		1.09×10^5 ($\pm 0.51 \times 10^5$)	5.69×10^{-3} ($\pm 1.35 \times 10^{-3}$)	70.1 (±24.9)	
uPA-SerpinB2^{KYK}	Heterogeneous analyte	2.01×10^4 ($\pm 0.22 \times 10^4$)	3.7×10^{-5} ($\pm 2.11 \times 10^{-5}$)	1.53 (±0.43)	4.3
		1.66×10^5 ($\pm 0.33 \times 10^5$)	3.35×10^{-3} ($\pm 1.05 \times 10^{-3}$)	51.2 (±12.9)	
uPA-SerpinE1	Heterogeneous analyte	9.01×10^4 ($\pm 1.5 \times 10^4$)	1.65×10^{-5} ($\pm 0.19 \times 10^{-3}$)	1.48 (±0.30)	9.4
		3.55×10^5 ($\pm 0.33 \times 10^5$)	0.98×10^{-3} ($\pm 0.44 \times 10^{-3}$)	49.5 (±12.6)	

of uPA-SerpinB2^{YK} was increased to a level comparable with that of uPA-SerpinE1 (~7-fold compared with uPA alone) (Fig. 4*A*). The uPA-SerpinB2^{KYK} complex had no significant impact on endocytosis over and above that of uPA-SerpinB2^{YK} (Fig. 4*A*). This result reflected the similar VLDLR binding affinities of these two complexes (Table 1) and further confirms that completion of the LDLR-binding motif is necessary and sufficient for enhanced endocytosis via VLDLR.

Further investigation of endocytosis in an LRP1-dependent cell model (PC-3) showed that the LDLR-binding motif alone

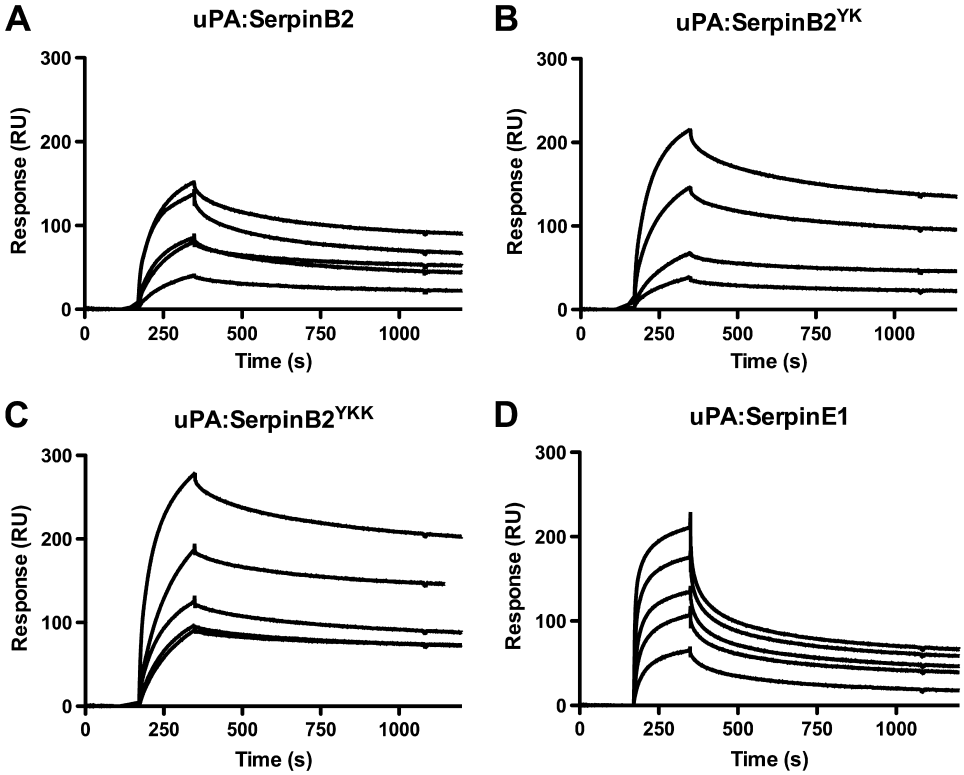

FIGURE 3. **Surface plasmon resonance analysis of the interaction between uPA-Serpin complexes and LRP1.** Surface plasmon resonance analysis of the dose-dependent interaction between LRP1 and uPA complexed SerpinB2 mutants as indicated (*A–C*) and uPA complexed SerpinE1 (*D*). The data presented here are representative of at least three experiments with analyte concentrations from 100 to 6.25 nM. All of the SerpinB2 forms were constructed on the SerpinB2 ΔCD-loop backbone.

TABLE 2

Kinetic parameters of the interaction between Serpin forms used in this study and the endocytosis receptor LRP1

The values were determined using surface plasmon resonance. The binding data were fitted using BIAevaluation 4.0 software. The binding model chosen represents that with the lowest χ^2 value. (The values are the averages ± S.E., $n \geq 3$). All of the SerpinB2 forms were constructed on the SerpinB2 ΔCD-loop backbone.

Analyte	Binding model	k_a	k_d	K_D	χ^2
		$M^{-1}\,s^{-1}$	s^{-1}	nM	
uPA-SerpinE1	Heterogeneous analyte	9.52×10^4 ($\pm 2.89 \times 10^4$)	2.68×10^{-5} ($\pm 0.84 \times 10^{-5}$)	0.252 (±0.087)	8.31
		6.09×10^5 ($\pm 1.56 \times 10^5$)	1.30×10^{-3} ($\pm 0.33 \times 10^{-3}$)	2.13 (±0.56)	
uPA-SerpinB2	1:1	6.74×10^4 ($\pm 4.53 \times 10^4$)	6.71×10^{-4} ($\pm 1.32 \times 10^{-4}$)	1.02 (±0.54)	3.41
uPA-SerpinB2^{YK}	Heterogeneous analyte	1.38×10^5 ($\pm 0.48 \times 10^5$)	1.9×10^{-5} ($\pm 0.87 \times 10^{-5}$)	0.808 (±0.246)	3.35
		1.24×10^5 ($\pm 0.44 \times 10^5$)	8.06×10^{-3} ($\pm 7.41 \times 10^{-3}$)	57.8 (±39.0)	
uPA-SerpinB2^{YKK}	Heterogeneous analyte	3.43×10^5 ($\pm 1.34 \times 10^5$)	3.68×10^{-5} ($\pm 1.67 \times 10^{-5}$)	0.128 (±0.081)	7.32
		1.97×10^5 ($\pm 1.39 \times 10^5$)	1.10×10^{-2} ($\pm 1.55 \times 10^{-2}$)	2.72 (±1.51)	

was not sufficient for enhanced endocytosis via LRP1. Although a small but significant increase in RAP-sensitive uPA-SerpinB2 endocytosis was observed compared with uPA alone, no significant difference in internalization was observed between uPA-SerpinB2 and uPA-SerpinB2^{YK} (Fig. 4*B*). However, the levels of uPA-SerpinB2^{YKK} and uPA-SerpinE1 endocytosis were similarly significantly enhanced ~2.5-fold compared with uPA alone and ~1.6-fold compared with uPA-SerpinB2 (Fig. 4*B*). These functional data are entirely consistent with the biochemical data describing the differential interactions of uPA-SerpinB2^{YK} *versus* uPA-SerpinB2^{YKK} with LRP1 (Table 2).

Introduction of VLDLR Binding to SerpinB2 Induces Mitogenic Signaling in MCF-7 Cells—As observed previously (21, 23), the increased ERK phosphorylation in breast cancer cells by uPA-SerpinE1 compared with uPA is not observed in cells treated with uPA-SerpinB2 (Fig. 5*A*), and this effect is potentially caused by a lack of a LDLR minimal binding motif in SerpinB2. The importance of an intact LDLR minimal binding motif in facilitating this activity was confirmed, because stimulation of MCF-7 cells with uPA-SerpinB2^{YK} initiated a significant increase in ERK phosphorylation (~3.5-fold within 3 min, relative to uPA alone) (Fig. 5*A*). The kinetics of ERK phosphorylation was similar to that observed for uPA-SerpinE1. Furthermore, a correlation ($R^2 = 0.9790$) was observed between VLDLR affinity and ERK phosphorylation after 3 min of treatment (Fig. 5*B*).

A downstream functional outcome of sustained ERK phosphorylation in MCF-7 cells stimulated by uPA-SerpinE1 is induction of proliferation (21, 23). Thus, we measured the effect of uPA-SerpinB2^{YK} on MCF-7 cell proliferation in real time using the xCELLigence system (Fig. 5, *C* and *D*). Cell indices for uPA-SerpinB2^{YK} and uPA-SerpinE1 treatments were distinct from those observed for cells incubated with uPA or uPA-SerpinB2 (Fig. 5*C*). Clear proliferative effects were evident over an extended time frame following the addition of either uPA-SerpinB2^{YK} or uPA-SerpinE1, as reflected in an apparent loga-

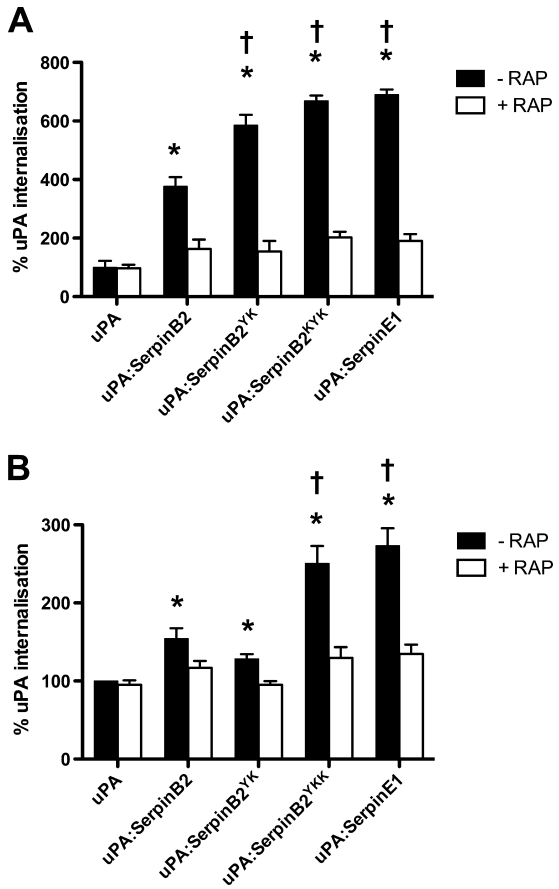

FIGURE 4. **Increased LDLR affinity leads to increased internalization of uPA-Serpin complexes by cancer cells.** *A*, MCF-7 cells were incubated in the presence or absence of RAP (200 nM) for 15 min at 37 °C, prior to analysis of internalization of Alexa 488-labeled uPA by fluorescence quenching assay. The values are the means ± S.E. ($n = 3$). *B*, PC-3 cells were incubated in the presence or absence of RAP (200 nM) for 15 min at 37 °C prior to analysis of internalization of Alexa 488-labeled uPA by fluorescence quenching assay. The values are the means ± S.E. ($n = 3$). *, $p < 0.005$ compared with relative uPA treatment; †, $p < 0.005$ compared with relative uPA-SerpinB2 treatment. All of the SerpinB2 forms were constructed on the SerpinB2 ΔCD-loop backbone.

rithmic phase growth pattern (Fig. 5*C*). This resulted in a significant (~1.6-fold) increase in cell index relative to controls (media, uPA, or uPA-SerpinB2) after 72 h (Fig. 5*D*). Interestingly, cell indices following uPA-SerpinB2^{YK} or uPA-SerpinE1 treatment were initially slightly lower than those obtained following treatment with uPA or uPA-SerpinB2. No difference was observed between cells incubated with uPA or uPA-SerpinB2 (Fig. 5, *C* and *D*), with both reaching a plateau between 12 and 36 h post-treatment before declining, suggesting a decrease in cell number.

DISCUSSION

This study provides the first molecular characterization of key structural elements that define the differential interactions of SerpinE1 and SerpinB2 with LDLR receptors and their functional implications for downstream mitogenic signaling and cell proliferation. Completion of the LDLR-binding motif in SerpinB2 to match a corresponding motif in SerpinE1 complemented SerpinB2 activity with the promitogenic function of SerpinE1 (when complexed with uPA). Thus, we suggest that the high LDLR binding affinity and endocytosis rate of uPA-SerpinE1 are part of the repertoire of effects attributable to the promitogenic function of SerpinE1. This partly explains why, despite a shared serpin inhibitory function, high tumor levels of uPA and SerpinE1 promote tumor progression, whereas high levels of SerpinB2 are protective (10).

We and others have previously reported the existence of a strong correlation between the affinity of uPA-Serpin complexes for VLDLR and uPA-Serpin endocytosis (21, 23) and suggested that VLDLR affinity may be the rate-limiting determinant of uPA/uPAR clearance from the cell surface (21). In comparison with uPA-SerpinE1, the uPA-SerpinB2^{YK} complex displayed similar binding affinity to VLDLR and was internalized via this endocytosis receptor in a similar manner. The importance of the LDLR-binding motif in increasing the VLDLR binding affinity and enhanced endocytosis was confirmed by the lack of a significant impact of uPA-SerpinB2^{KYK} over and above that of uPA-SerpinB2^{YK}. Because members of the LDLR family have overlapping yet distinct ligand specificities (33), the presence of the LDLR minimal binding motif alone was not sufficient to introduce binding to LRP1. Skeldal *et al.* (24) reported that Lys^{88} was critical for the interaction of SerpinE1 with LRP1. Consistent with this, modification of Asn^{120} in SerpinB2 (corresponding to Lys^{88} in SerpinE1), in conjunction with a complete LDLR minimal binding motif, produced a SerpinB2 form (*i.e.* SerpinB2^{YKK}) with LRP1 binding kinetics and LRP1-mediated endocytosis similar to those of uPA-SerpinE1. These observations confirm that LDLR affinity is the rate-limiting step of uPA-Serpin endocytosis.

Webb *et al.* (23) demonstrated that the affinity of uPA-Serpin complexes for VLDLR is correlated with sustained activation of ERK and increased cell proliferation in MCF-7 cells. We have now shown that SerpinB2 function can be complemented with the VLDLR binding and downstream functional activity associated with SerpinE1 by completion of the LDLR minimal binding motif within α-helix D. As such, it is clear that VLDLR affinity is the key property underlying the differences in ERK activation and subsequent effects on cell proliferation between uPA-SerpinE1 and uPA-SerpinB2. Given this, it was unnecessary to investigate the impact of uPA-SerpinB2^{KYK} (or other SerpinB2 mutants generated with incomplete LDLR-binding motifs) on mitogenic signaling, because the VLDLR binding affinity of this complex was indistinguishable from that of uPA-SerpinB2^{YK}. Direct binding of SerpinE1 to LRP1 has also been demonstrated to activate the JAK/STAT pathway, leading to increased cell motility (34). However, because the prognostic data for SerpinE1 is only significant in tumors also expressing uPA (1–3, 35), the impact of complementing SerpinB2 with LRP1 binding on the activation of this pathway was not investigated in this study.

Although high affinity binding of uPA-Serpin complexes to VLDLR is clearly vital for the induction of downstream ERK activation, it is important to note that high affinity binding of any ligand to VLDLR will not necessarily induce the same response. This is particularly highlighted by the high affinity interaction of RAP with VLDLR ($K_D = 0.7$ nM) (36), which fails to induce downstream ERK activation and cell proliferation (21, 23). Therefore, the rapid formation of a multimolecular com-

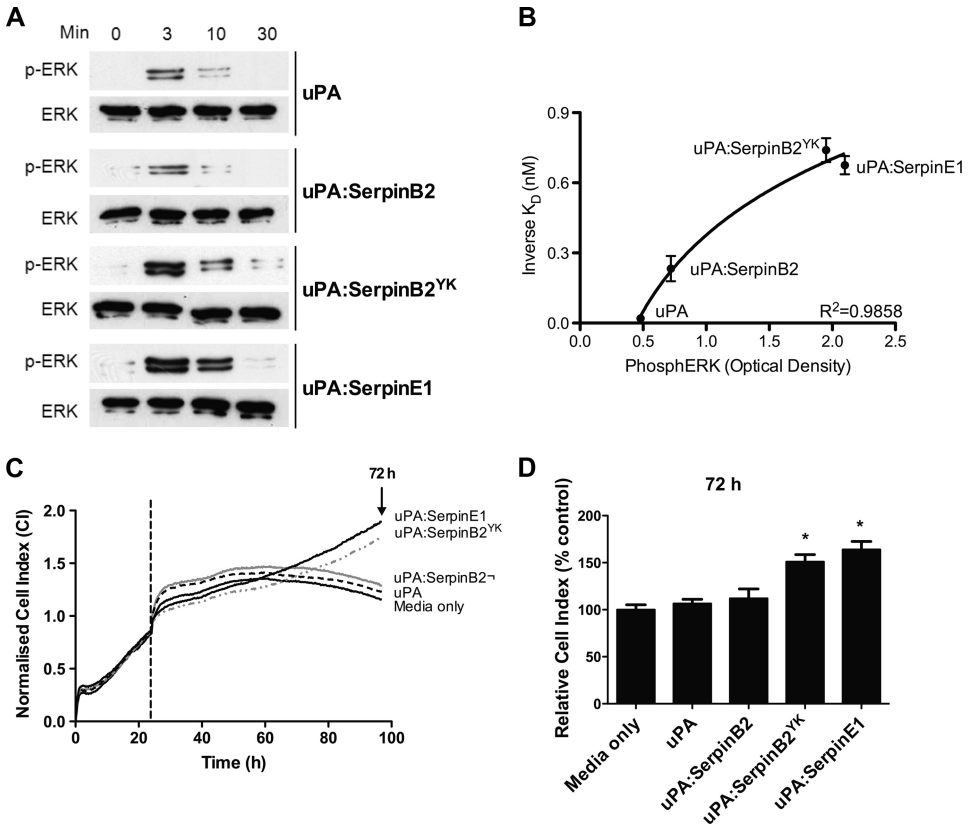

FIGURE 5. **uPA-SerpinB2^{YK} induces promitogenic signaling pathways and increased cell proliferation in MCF-7 cells similar to those of uPA-SerpinE1.** *A*, MCF-7 cells were cultured in serum-free medium for 12 h and then exposed to 5 nM uPA, uPA-SerpinB2, uPA-SerpinB2^{YK}, or uPA-SerpinE1 for the indicated times. The cell lysates were analyzed for phosphorylated and total ERK by Western blotting. *B*, levels of phosphorylated ERK after 3 min of stimulation with 10 nM uPA, uPA-SerpinB2, uPA-SerpinB2^{YK}, or uPA-SerpinE1 were correlated with the affinity of each ligand for VLDLR (Table 1). The data were fitted to a logarithmic equation using GraphPad Prism v5.00 (GraphPad Software, San Diego, CA). *C*, MCF-7 cells were cultivated in E-plates with RPMI with 5% FCS for 24 h, before changing to serum-free medium containing 10 nM uPA, uPA-SerpinB2, uPA-SerpinB2^{YK}, uPA-SerpinE1, or medium only, and cell proliferation was monitored over 72 h in real time using an xCELLigence RTCA DP system. The electronic readout of cell sensor impedance is displayed continuously as the cell index (*CI*) normalized to the compound addition time point (indicated by a *vertical dotted line*). The cell index value at each time point is defined as $(R_n - R_b)/R_b$, where R_n is the electrode impedance of wells with cells, and R_b is the background of wells with media alone. The curves are the means of four replicates. *D*, bar graph showing CI values 72 h after the addition of proteins as percentages of medium only treatment (72-h treatment time point is indicated on electronic readout by *arrow* in *C*). The values are the means ± S.E. ($n = 4$). *, $p < 0.005$ compared with medium only control. All of the SerpinB2 forms were constructed on the SerpinB2 ΔCD-loop backbone.

plex consisting of VLDLR, a uPA-Serpin complex, uPAR, and any associated integrins or coreceptors is likely necessary for the induction of this signal, not merely the recognition of a high affinity ligand by VLDLR alone.

Other factors that may impact on the prognostic differences between overexpression of SerpinE1 *versus* SerpinB2 in cancer include the complex interplay of interactions between uPA/uPAR, SerpinE1, and other ligands and coreceptors, through which SerpinE1 modulates adhesion and migration. For example, in the context of cell adhesion, SerpinE1 competes with uPAR and integrins for vitronectin binding (10, 37, 38), but SerpinB2 does not bind vitronectin (39). Importantly, the vitronectin-binding site(s) in SerpinE1 are distinct from the LDLR minimal binding motif (40), and the SerpinB2 constructs used in this study did not bind to vitronectin or impact on cell adhesion (data not shown). This excludes any influence of modulation of cell adhesion on the proliferative effects of SerpinB2^{YK} on a VLDLR-dependent cell line and implies that these effects are a direct response of the increased affinity for VLDLR. Regardless, the absence of an LDLR minimal binding motif in the SerpinB2 moiety of uPA-SerpinB2 complex suggests a mechanism where, unlike SerpinE1, extracellular SerpinB2 could inhibit and clear cellular uPA, thereby preventing plasmin-mediated ECM degradation, without inducing cell proliferation.

In conclusion, this study clearly demonstrates that VLDLR affinity is the critical determinant underlying the disparate roles of SerpinE1 and SerpinB2 in mitogenic signaling and cell proliferation. Understanding the molecular basis of such physiological roles provides a mechanistic basis for the association of these proteins with disease severity and outcome and provides a sound rationale for potential therapeutic development.

REFERENCES

1. Foekens, J. A., Peters, H. A., Look, M. P., Portengen, H., Schmitt, M., Kramer, M. D., Brünner, N., Jänicke, F., Meijer-van Gelder, M. E., Henzen-Logmans, S. C., van Putten, W. L., and Klijn, J. G. (2000) *Cancer Res.* **60,** 636–643
2. Duffy, M. J. (2004) *Curr. Pharm. Des.* **10,** 39–49
3. Choong, P. F., and Nadesapillai, A. P. (2003) *Clin. Orthop. Relat. Res.* **415,** S46–S58
4. Duffy, M. J., Maguire, T. M., McDermott, E. W., and O'Higgins, N. (1999) *J. Surg. Oncol.* **71,** 130–135

5. Scherrer, A., Wohlwend, A., Kruithof, E. K., Vassalli, J. D., and Sappino, A. P. (1999) *Br. J. Haematol.* **105,** 920–927
6. Schmitt, M., Wilhelm, O. G., Reuning, U., Krüger, A., Harbeck, N., Lengyel, E., Graeff, H., Gänsbacher, B., Kessler, H., Bürgle, M., Stürzebecher, J., Sperl, S., and Magdolen, V. (2000) *Fibrinolysis Proteol.* **14,** 114–132
7. Weigelt, B., Peterse, J. L., and van't Veer, L. J. (2005) *Nat. Rev. Cancer* **5,** 591–602
8. Look, M. P., van Putten, W. L., Duffy, M. J., Harbeck, N., Christensen, I. J., Thomssen, C., Kates, R., Spyratos, F., Fernö, M., Eppenberger-Castori, S., Sweep, C. G., Ulm, K., Peyrat, J. P., Martin, P. M., Magdelenat, H., Brünner, N., Duggan, C., Lisboa, B. W., Bendahl, P. O., Quillien, V., Daver, A., Ricolleau, G., Meijer-van Gelder, M. E., Manders, P., Fiets, W. E., Blankenstein, M. A., Broët, P., Romain, S., Daxenbichler, G., Windbichler, G., Cufer, T., Borstnar, S., Kueng, W., Beex, L. V., Klijn, J. G., O'Higgins, N., Eppenberger, U., Jänicke, F., Schmitt, M., and Foekens, J. A. (2002) *J. Natl. Cancer Inst.* **94,** 116–128
9. Harris, L., Fritsche, H., Mennel, R., Norton, L., Ravdin, P., Taube, S., Somerfield, M. R., Hayes, D. F., and Bast, R. C., Jr. (2007) *J. Clin. Oncol.* **25,** 5287–5312
10. Croucher, D. R., Saunders, D. N., Lobov, S., and Ranson, M. (2008) *Nat. Rev. Cancer* **8,** 535–545
11. Bouchet, C., Hacène, K., Martin, P. M., Becette, V., Tubiana-Hulin, M., Lasry, S., Oglobine, J., and Spyratos, F. (1999) *J. Clin. Oncol.* **17,** 3048–3057
12. D'Alessio, S., and Blasi, F. (2009) *Front. Biosci.* **14,** 4575–4587
13. Preissner, K. T., Kanse, S. M., and May, A. E. (2000) *Curr. Opin. Cell Biol.* **12,** 621–628
14. Resnati, M., Pallavicini, I., Wang, J. M., Oppenheim, J., Serhan, C. N., Romano, M., and Blasi, F. (2002) *Proc. Natl. Acad. Sci. U.S.A.* **99,** 1359–1364
15. Strickland, D. K., and Ranganathan, S. (2003) *J. Thromb. Haemostasis* **1,** 1663–1670
16. Astedt, B., Lecander, I., and Ny, T. (1987) *Fibrinolysis* **1,** 203–208
17. Ellis, V., Wun, T. C., Behrendt, N., Rønne, E., and Danø, K. (1990) *J. Biol. Chem.* **265,** 9904–9908
18. Al-Ejeh, F., Croucher, D., and Ranson, M. (2004) *Exp. Cell Res.* **297,** 259–271
19. Argraves, K. M., Battey, F. D., MacCalman, C. D., McCrae, K. R., Gåfvels, M., Kozarsky, K. F., Chappell, D. A., Strauss, J. F., 3rd, and Strickland, D. K. (1995) *J. Biol. Chem.* **270,** 26550–26557
20. Croucher, D., Saunders, D. N., and Ranson, M. (2006) *J. Biol. Chem.* **281,** 10206–10213
21. Croucher, D. R., Saunders, D. N., Stillfried, G. E., and Ranson, M. (2007) *Biochem. J.* **408,** 203–210
22. Di, Y., Liu, Z., Tian, J., Zong, Y., Yang, P., and Qu, S. (2010) *FEBS Lett.* **584,** 3469–3473
23. Webb, D. J., Thomas, K. S., and Gonias, S. L. (2001) *J. Cell Biol.* **152,** 741–752
24. Skeldal, S., Larsen, J. V., Pedersen, K. E., Petersen, H. H., Egelund, R., Christensen, A., Jensen, J. K., Gliemann, J., and Andreasen, P. A. (2006) *FEBS J.* **273,** 5143–5159
25. Stefansson, S., Muhammad, S., Cheng, X. F., Battey, F. D., Strickland, D. K., and Lawrence, D. A. (1998) *J. Biol. Chem.* **273,** 6358–6366
26. Horn, I. R., van den Berg, B. M., Moestrup, S. K., Pannekoek, H., and van Zonneveld, A. J. (1998) *Thromb. Haemostasis* **80,** 822–828
27. Rodenburg, K. W., Kjoller, L., Petersen, H. H., and Andreasen, P. A. (1998) *Biochem. J.* **329,** 55–63
28. Jensen, G. A., Andersen, O. M., Bonvin, A. M., Bjerrum-Bohr, I., Etzerodt, M., Thøgersen, H. C., O'Shea, C., Poulsen, F. M., and Kragelund, B. B. (2006) *J. Mol. Biol.* **362,** 700–716
29. Cochran, B. J., Gunawardhana, L. P., Vine, K. L., Lee, J. A., Lobov, S., and Ranson, M. (2009) *BMC Biotechnol.* **9,** 43
30. Aertgeerts, K., De Bondt, H. L., De Ranter, C. J., and Declerck, P. J. (1995) *Nat. Struct. Biol.* **2,** 891–897
31. Di Giusto, D. A., Sutherland, A. P., Jankova, L., Harrop, S. J., Curmi, P. M., and King, G. C. (2005) *J. Mol. Biol.* **353,** 1069–1080
32. Ehrlich, H. J., Gebbink, R. K., Keijer, J., and Pannekoek, H. (1992) *J. Biol. Chem.* **267,** 11606–11611
33. Strickland, D. K., Gonias, S. L., and Argraves, W. S. (2002) *Trends Endocrinol. Metab.* **13,** 66–74
34. Degryse, B., Neels, J. G., Czekay, R. P., Aertgeerts, K., Kamikubo, Y., and Loskutoff, D. J. (2004) *J. Biol. Chem.* **279,** 22595–22604
35. Ohba, K., Miyata, Y., Kanda, S., Koga, S., Hayashi, T., and Kanetake, H. (2005) *J. Urol.* **174,** 461–465
36. Battey, F. D., Gåfvels, M. E., FitzGerald, D. J., Argraves, W. S., Chappell, D. A., Strauss, J. F., 3rd, and Strickland, D. K. (1994) *J. Biol. Chem.* **269,** 23268–23273
37. Stefansson, S., McMahon, G. A., Petitclerc, E., and Lawrence, D. A. (2003) *Curr. Pharm. Des.* **9,** 1545–1564
38. Deng, G., Royle, G., Wang, S., Crain, K., and Loskutoff, D. J. (1996) *J. Biol. Chem.* **271,** 12716–12723
39. Mikus, P., Urano, T., Liljeström, P., and Ny, T. (1993) *Eur. J. Biochem.* **218,** 1071–1082
40. Jensen, J. K., Wind, T., and Andreasen, P. A. (2002) *FEBS Lett.* **521,** 91–94